Journal of Magnetic Resonance 196 (2009) 115–118

Contents lists available at ScienceDirect

Journal of Magnetic Resonance

journal homepage: www.elsevier.com/locate/jmr

Generating spin turbulence through nonlinear excitation in liquid-state NMR

Daniel Abergel [a,*], Alain Louis-Joseph [b]

[a] Département de Chimie, Ecole Normale Supérieure, 24, rue Lhomond, 75231 Paris Cedex 05, France
[b] ICSN-RMN, Ecole Polytechnique 91128 Palaiseau Cedex, France

ARTICLE INFO

Article history:
Received 2 September 2008
Revised 13 October 2008
Available online 26 October 2008

Keywords:
NMR
Radiation damping
Chaos
Nonlinearity
Spin turbulence

ABSTRACT

Chaotic dynamics of a water magnetization in a 600 MHz NMR spectrometer was generated by a radiation damping-based electronic feedback. Erratic induction signal was observed for *several tens of seconds*. The analysis of the data shows that this chaotic behaviour can be ascribed to spin turbulence in the sample and that a simpler model based on the three-dimensional Bloch equations modified to include a feedback field may not account for the experimental data.

1. Introduction

The dynamics of a system of uncoupled spins can be described in terms of the classical Bloch equations or alternatively within the framework of quantum mechanics by the use of the Liouville equation for the density operator [1]. Both approaches cover most cases of interest and provide extremely powerful tools for understanding and predicting spin dynamics. However, at high magnetic fields, radiation damping, which originates from the interaction between the NMR circuitry and the spins, is no longer negligible and this conventional description must be modified. The practical consequences of radiation damping are well known. It can alter the dynamics of the water magnetization and lead to poor suppression of the water signal [2]. It is also responsible for the occurence of multiquantum-like peaks in various 2D experiments [3–5], and has been recently proposed as a mechanism of contrast enhancement in magnetic resonance imaging [6].

In another context, typical nonlinear behaviour of the magnetization can be generated by using a radiation damping-based electronic feedback device to modulate and control radiation damping. Thus, inverting the effects of the radiation damping field was recently demonstrated to generate self-sustained periodic maser pulses [7]. Moreover, the possible appearance of a chaotic behaviour of the magnetization in this context was suggested by numerical simulations of the nonlinear Bloch equations (NLBE), obtained from the Bloch equations by adding the relevant feedback field [8]. In addition, recent observations illustrate the potential complexity of the magnetization dynamics in high field NMR spectrometers caused by demagnetizating field effects and/or radiation damping on water magnetization [9] or hyperpolarized spins [10]. In this paper, we present our observations of stationary chaotic behaviour of a large magnetization in high resolution liquid state NMR, through back-action from the probe, and that can be interpreted in terms of spin turbulence.

2. Results

Experiments were performed on a Bruker DRX600 MHz spectrometer equipped with the Radiation Damping Control Unit (RDCU) hardware based on the authors' prototype and a high Q TXI probe with Oz gradient facility. Nonlinear excitation of the magnetization was achieved by feeding into the probe a radiofrequency field obtained from a fraction of the residual water signal, with appropriate phase and gain adjustment, as detailed elsewhere [11,12]. After optimum tuning and matching of the probe, amplitude and phase of the RDCU were adjusted for cancellation of radiation damping [12]. The sample consisted of 90% H_2O and 10% D_2O. A typical experiment started with a hard pulse to create in-plane magnetization. It was then followed by signal acquisition during which feedback excitation was active. The duration of the aquisition was significantly longer (32 s) than usual liquid state NMR observation times, which allowed to capture typical nonlinear behaviour originating from the interplay between nonlinear excitation and water spin–lattice relaxation [7]. The radiation damping time was estimated by measuring the linewidths of the water resonance after a small angle pulse, with the probe tuned and detuned, respectively. It was found to be on the order of

* Corresponding author. Fax: +33 1 44 32 33 97.
E-mail address: daniel.abergel@ens.fr (D. Abergel).

1090-7807/$ - see front matter © 2008 Elsevier Inc. All rights reserved.
doi:10.1016/j.jmr.2008.10.016

$\tau_{RD} \approx 27$ ms. With this experimental setup, induction signals exhibited self-sustained maser pulses for sufficient feedback gains. In Fig. 1(a), the feedback power used was 10 dB stronger than that needed for the suppression of radiation damping and the feedback phase was adjusted for the suppression of radiation damping ($\psi = \pi/2$ in Eq. (4) below). For higher feedback gains, i.e., for more intense feedback fields, erratic motion could be generated. Signals obtained for three increasing values of the feedback gain are represented in Fig. 1(a)–(c)), and illustrate the transition from regular to chaotic regime of the magnetization. The FID trace on the upper part of the figure shows the regular appearance of maser bursts. These bursts have identical amplitudes and are separated by a nearly constant time interval of several seconds. Alternatively, for increasing feedback field intensities, the observed signal exhibits irregular bursts of magnetization, with different profiles and occurring at irregularly spaced intervals. Note that the intensities of these maser bursts are significantly lower than in the case of regular motion, which is due to the saturation of the magnetization by a larger rf feedback rf power. It is seen that the further increase of the FB field induces even more irregularities of the bursts, both in terms of shaps and delays of occurence. This chaotic process goes on through the total duration of the observation window and it is therefore likely that the magnetization has reached a steady state.

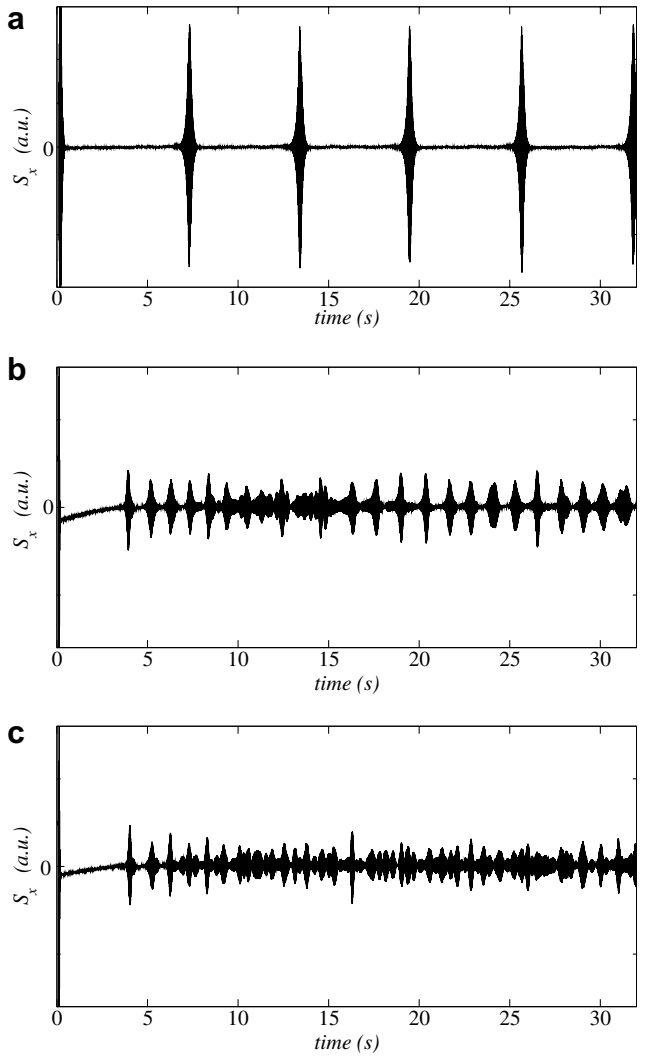

Fig. 1. Transition to chaotic motion of the detected signal. In (a), the motion is regular, exhibiting self-sustained oscillations; in (b), bursts of chaotic motion are superimposed to a background regular behaviour; while in (c) completely irregular motion is observed.

2.1. Embedding measurements

In order to get some insight into the dynamics, an analysis of the steady state solution of the observed signal, considered as a dynamical system, was performed. In mathematical terms, the aim is to extract information about the manifold on which the magnetization vector evolves at long times. In usual situations, where the magnetization relaxes to equilibrium, the so-called attractor is a fixed point, namely, the North pole of the Bloch sphere. Alternatively, for a nutation experiment where relaxation is neglected, the steady state is a closed orbit, therefore of dimension one. In the case of chaotic behaviour, the attractor does not have an integer dimension (for general references, see for instance [13–15]). Thus, one of the ways to characterize an attractor is to estimate its correlation dimension D_2 from the observed signal [16], defined as:

$$D_2 = \lim_{r\to 0} \log C(r)/\log r, \tag{1}$$

where the correlation integral $C(r)$ of an n-dimensional dynamical system is [16]:

$$C(r) = \lim_{N\to\infty} C(N,r) = \lim_{N\to\infty} \frac{1}{N(N-1)} \sum_{i\neq j=1}^{N} \Theta(r - \|\mathbf{x}_i^{(n)} - \mathbf{x}_j^{(n)}\|), \tag{2}$$

In Eq. (2), Θ is the Heaviside step function and N is the number of points in the time series. The quantity $C(r)$ represents the probability that two points $\mathbf{x}_i^{(n)}$ and $\mathbf{x}_j^{(n)}$ on the attractor are separated by a distance smaller than r. It can be shown that the dimension of the attractor of the original dynamical system can be calculated by using the $n-$dimensional delay coordinate representation of the observed NMR signal [13,17,18]: $\{M(t), M(t-\tau), \ldots, M(t-(n-1)\tau)\}$, where $M(t)$ is a function of the observed signal, the magnitude of the transverse magnetization in this case. The integer n is called the embedding dimension. Then, it can be shown [19] that the estimated dimension $D_2^{(n)}$ for an embedding dimension n is $D_2^{(n)} = n$ for $n < D_2$ (since in this case the attractor is projected onto a space of lower dimension) and reaches a constant value $D_2^{(n)} = D_2$ for $n \geqslant ceil(D_2)$.

We used this approach to estimate the correlation dimension of the chaotic attractor of the magnetization from experimental measurements. Calculations were carried out with the TISEAN software [20]. As this estimate may be flawed by various sources of errors analyzed at length in the literature [14], caution need be exercised when computing and interpreting results. Thus, the maximum dimension that can be calculated from a time series depends on the number of data points N, [21,22] which in our case was on the order of $N \approx 4.10^4$. We used the criterion proposed by Ruelle and Eckmann [22] that states that the maximum dimension that can be extracted from N data points is:

$$D_2^{max} = \frac{2\log N}{\log(1/\rho)} \tag{3}$$

where $\rho = r/R$ is the ratio of a typical value r in the scaling region, at which the slope is evaluated, and R is the diameter of the reconstructed attractor. Moreover, the value of r was taken as the midpoint between the upper and lower bounds in the scaling region: [23] $r = (r_{max} + r_{min})/2$ and the minimal length for slope determination was such that $\log r_{max} - \log r_{min} \geqslant 1.6$, which corresponds to a fivefold ratio in r.

Local slopes were calculated across the linear region [24], the mean and standard deviations of which provided the values $\langle D_2^{(n)} \rangle$ and $\sigma_{D_2^{(n)}}$. Results are depicted in Fig. 2, where the values of

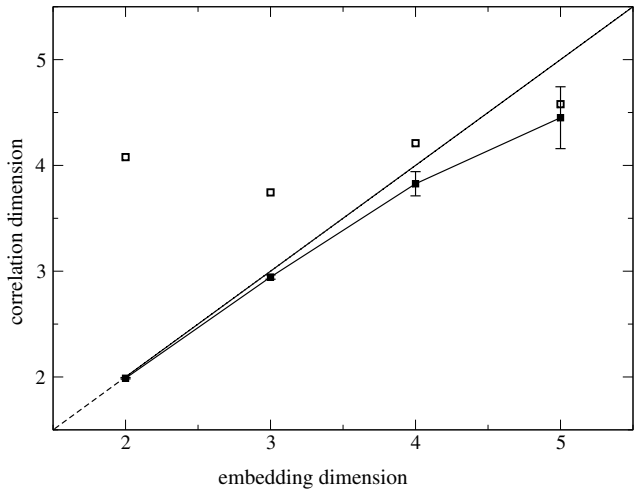

Fig. 2. Estimated correlation dimensions obtained from the data of Fig. 1 are depicted. The solid line corresponds to $\langle D_2^{(n)} \rangle$, the correlation dimension for embedding dimension n. In addition, the maximum acceptable values of D_2 compatible with the data used are plotted as open squares ($D_{max}^{(n)}$).

the dimensions $\langle D_2^{(n)} \rangle$ (solid line and filled squares) are plotted together with the maximum significant value $D_{max}^{(n)}$ (open squares). It is seen that for embedding dimensions as large as $n = 5$, the values $\langle D_2^{(n)} \rangle$ lie below the maximum achievable dimension. Therefore, the present analysis of the experimental data provides unambiguous evidence that the attractor dimension is strictly larger than $D_2 = 4$. However, no definite conclusion can be drawn for higher embedding dimensions, so that the size of the attractor could not be determined. This is in itself an interesting result, which demonstrates that the kind of dynamics generated by the setup cannot be interpreted in terms of the conventional three dimensional Bloch equations modified to account for the presence of the feedback field.

3. Discussion and conclusion

In order to interpret the presence of the erratic behaviour of the magnetization that was observed experimentally, we used a dynamical model that includes both feedback field effects and $\mathbf{B}_0$ inhomogeneity. In this model, inhomogeneities of the static field are not accounted for by a simple inhomogeneous line broadening. Rather, the magnetization is explicitly decomposed in isochromats $\boldsymbol{\mu}(\delta\omega)$, each of which evolves at a frequency determined by a Lorentzian resonance spread defined by $h(\delta\omega) = (1/\pi) \times R_2^{\dagger}/[R_2^{\dagger 2} + \delta\omega^2]$, where the inhomogeneous linewidth R_2^* is given by $R_2^* = R_2 + R_2^{\dagger}$, and R_2 is the homogeneous transverse relaxation rate of the spins. Thus, each magnetization component $\boldsymbol{\mu}(\delta\omega)$ evolving at the Larmor frequency offset $\delta\omega$ undergoes the cumulative action of the individual feedback fields generated by the spins associated with all the isochromats in the sample. Each of the $\boldsymbol{\mu}(\delta\omega)$ is coupled to the probe such that it generates a back action field:

$$B_{FB}(\delta\omega) = G\mu_t(\delta\omega)e^{-i\psi}, \tag{4}$$

where $\mu_t(\delta\omega) = \mu_x(\delta\omega) + i\,\mu_y(\delta\omega)$. The coupling parameters G and ψ are identical for all the isochromats and in the case of radiation damping, they are equal to $\psi = -\pi/2$ and $G = \mu_0\eta Q/2$ in SI units, where μ_0 is the vacuum permitivity and Q is the quality factor of the probe. In the absence of an applied radiofrequency B_1 field, the evolution equations in the rotating frame are: [7]

$$\begin{cases} \dfrac{d}{dt}\mu_x(\delta\omega) = \delta\omega\ \mu_y(\delta\omega) - \mu_z(\delta\omega)\Omega_{FB,y} - R_2\mu_x(\delta\omega) \\ \dfrac{d}{dt}\mu_y(\delta\omega) = -\delta\omega\ \mu_x(\delta\omega) + \mu_z(\delta\omega)\Omega_{FB,x} - R_2\mu_y(\delta\omega) \\ \dfrac{d}{dt}\mu_z(\delta\omega) = \mu_x(\delta\omega)\Omega_{FB,y} - \mu_y(\delta\omega)\Omega_{FB,x} - R_1(\mu_z(\delta\omega) - \mu_0(\delta\omega)) \end{cases} \tag{5}$$

In Eq. (5), one has $\boldsymbol{\Omega}_{FB} = \gamma\mathbf{B}_{FB}$ and:

$$\mathbf{B}_{FB} = G\begin{pmatrix} sin\psi \int_{-\infty}^{\infty} \mu_y(\delta\omega)d(\delta\omega) + cos\psi \int_{-\infty}^{\infty} \mu_x(\delta\omega)d(\delta\omega) \\ -sin\psi \int_{-\infty}^{\infty} \mu_x(\delta\omega)d(\delta\omega) + cos\psi \int_{-\infty}^{\infty} \mu_y(\delta\omega)d(\delta\omega) \\ 0 \end{pmatrix}. \tag{6}$$

Eq. (5) served as the basis of the interpretation of self-sustained maser pulses observed previously [7,25].

This representation is similar to the one appearing in the work of Augustine and Hahn [26], generalized here to the case of a feedback field of arbitrary phase and gain. Note that writing Eq. (6) one has implicitly assumed that the coupling of all the isochromats to the probe are identical. This can be expected for feedback fields larger than the spread in Larmor frequencies of the water spins, which is likely in our experiments where the feedback field was typically larger than the actual radiation damping field by a factor of ≈100.

In the quest for an interpretation of the observed chaotic FIDs, we simulated the evolution of a magnetization initially close to inversion (after a preparation pulse with a flip angle 0.95π), for different values of the feedback field coupling, or gain, G, whilst the phase ψ was set to $+\pi/2$, which permits to suppress or invert the radiation damping field. To avoid artefactual periodicity of the discretized version of Eqs. (5) and (6), simulations were performed with a frequency step $\delta\omega_i$ such that $\delta\omega \times t_{max} < 1$, where $t_{max} \approx 27\ s$ is the duration of the simulation. This implied the use of 701 isochromats in the calculations. Note that the number of isochromats did not influence the outcome of the simulation, as long as the above condition was fulfilled. Relaxation rates were set to $R_1 = 1/3.3\ s^{-1}$, $R_2 = 1/2\ s^{-1}$, $R_2^{\dagger} = 1/0.14\ s^{-1}$.

Calculations were performed using the Scilab software [27]. Results presented in Fig. 3 illustrate the transition to chaos of the magnetization dynamics. Indeed, for moderate values of G, one observes the known self-sustained maser pulses mentioned above, whereas for higher gain values, one observes bursts of in-plane

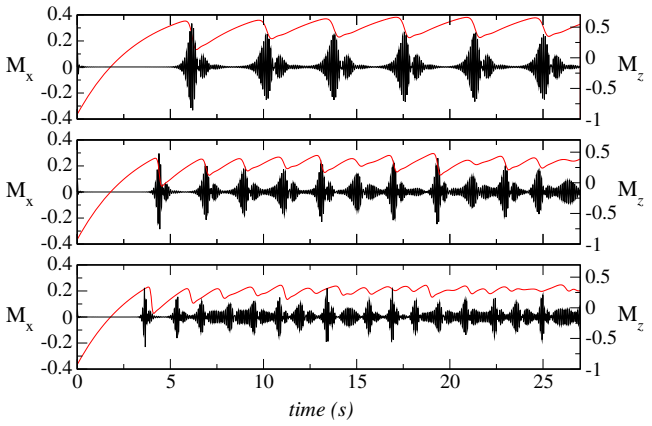

Fig. 3. Simulated M_x (black) and M_z (red) components of the magnetization for increasing values G of the feedback gain, illustrating the transition from a regular evolution made of self-sustained maser pulses (top) to a chaotic dynamics reflecting spin turbulence (center and bottom). (For interpretation of the references to colour in this figure legend, the reader is referred to the web version of this paper.)

magnetization that occur at irregular time intervals and have erratic shapes. With further increase of the gain (bottom), the FID becomes persistently chaotic in time. Thus, numerical simulations based on the model explicited by Eq. (5) are able to qualitatively reproduce our experimental observations. Of course, since dipolar field effects are not included in the model, one cannot expect to reproduce the details of the experimental time signals, and additional features may well be present, such as a supplementary frequency shift [28] of the maser pulses that adds to the one generated by the feedback field.

Recent work published in the literature have suggested the possibility to observe chaotic dynamics of the water magnetization in liquid state high-field NMR [9]. These effects were interpreted as the result of the interplay between radiation damping and the dipolar demagnetizing field. In that case, instability occurs transiently, and at time scales much shorter than the relaxation time T_1. More recently, Marion et al. [10] could observe stationary chaotic FIDs of dissolved hyperpolarized Xenon. Although both demagnetizing field effects and radiation damping were shown to be present, the experiments could nevertheless not be clearly interpreted in terms of these phenomena.

In the case in hand, combining experiments with numerical simulations that include a feedback field only and disregard dipolar field effects enables us to propose the model of the chaotic dynamics given by Eq. (5). Indeed, a simpler model based on the three dimensional nonlinear Bloch equations is ruled out by the fact that it would necessarily imply the existence of an attractor of dimension strictly smaller than 3 [29]. This is in contradiction with our analysis of the data, which showed that the attractor dimension was larger than 4. Therefore, our findings suggest that field inhomogeneities introduce nonlocality by making the dynamical system high (infinite) dimensional, which gives rise to spin turbulence.

References

[1] R.R. Ernst, G. Bodenhausen, A. Wokaun, Principles of Nuclear Magnetic Resonance in One and Two Dimensions, Oxford University Press, London, 1987.
[2] W.S. Price, Water signal suppression in NMR spectroscopy, Annual Reports on NMR Spectroscopy 38 (1999) 289–354.
[3] M. McCoy, W.S. Warren, Three-quantum nuclear magnetic resonance spectroscopy of liquid water—intermolecular multiple-quantum coherence generated by spin-cavity coupling, Journal of Chemical Physics 93 (1990) 858–860.
[4] D. Abergel, M.-A. Delsuc, J.-Y. Lallemand, Is ms multiple quantum nuclear magnetic resonance spectroscopy of liquid water real?, Journal of Chemical Physics 96 (1992) 1657–1658
[5] A. Vlassenbroek, J. Jeener, P. Broakaert, Radiation damping in high-resolution liquid NMR—a simulation study, Journal of Chemical Physics 103 (1995) 5886–5897.
[6] Contrast enhancement by feedback fields in magnetic resonance imaging, Journal of Physical Chemistry B 110 (2006) 2271–2278.
[7] D. Abergel, A. Louis-Joseph, J.-Y. Lallemand, Self-sustained maser oscillations of a large magnetization driven by a radiation damping-based electronic feedback, Journal of Chemical Physics 116 (2002) 7073–7080.
[8] D. Abergel, Chaotic solutions of the feedback driven Bloch equations, Physics Letters A 302 (2002) 17–22.
[9] Y.-Y. Lin, N. Lisitza, S. Ahn, W.S. Warren, Resurrection of crushed magnetization and chaotic dynamics in solution NMR spectroscopy, Science 290 (2000) 118–121.
[10] D.J. Marion, G. Huber, P. Berthault, H. Desvaux, Observation of noise-triggered chaotic emissions in an NMR-maser, ChemPhysChem 9 (2008) 1395–1401.
[11] A. Louis-Joseph, D. Abergel, J.-Y. Lallemand, Neutralization of radiation damping by selective feedback on a 400 MHz NMR spectrometer, J. Biomol. NMR 5 (1995) 212–216.
[12] D. Abergel, C. Carlotti, A. Louis-Joseph, J.-Y. Lallemand, Improvements in radiation damping control in high resolution NMR, J. Magn. Reson. B 109 (1995) 218–222.
[13] J.P. Eckmann, D. Ruelle, Ergodic theory of chaos and strange attractors, Rev. Mod. Phys. 57 (1985) 617–656.
[14] J. Theiler, Estimating fractal dimension, J. Opt. Soc. Am. A 7 (1990) 1055–1073.
[15] K.T. Alligood, T.D. Sauer, J.A. Yorke, Chaos: An Introduction to Dynamical Systems, Springer-verlag, New York, 1996.
[16] P. Grassberger, I. Procaccia, Characterization of strange attractors, Phys. Rev. Lett. 50 (1983) 346–349.
[17] N.H. Packard, J.P. Crutchfield, J.D. Farmer, R. Shaw, Geometry from a time series, Phys. Rev. Lett. 45 (1980) 712–716.
[18] F. Takens, Lecture Notes in Mathematics, Springer, Berlin, 1981.
[19] M. Ding, C.G.E. Ott, T. Sauer, J. Yorke, Plateau onset for correlation dimension—when does it occur, Phys. Rev. Lett. 70 (1993) 3872–3875.
[20] R. Hegger, H. Kantz, T. Schreiber, Chaos 9 (1999) 413–435.
[21] H.D.I. Abarbanel, R. Brown, J. Siderovitch, S. Tsimring, The analysis of observed chaotic data in physical systems, Rev. Mod. Phys. 65 (1993) 1331–1392.
[22] J.P. Eckmann, D. Ruelle, Fundamental limitations for estimating dimensions and lyapunov exponents in dynamic systems, Physica D 56 (1992) 185–187.
[23] P.E. Rapp, A. Albano, T. Schmah, L. Farwell, Filtered noise can mimic low-dimensional chaotic attractors, Phys. Rev. E 47 (1993) 2289–2297.
[24] G. Dori, S. Fishman, S.A. Ben-Haim, The correlation dimension of rat hearts in an experimentally controlled environment, Chaos 10 (2000) 257–267.
[25] A. Louis-Joseph, J.-Y. Lallemand, D. Abergel, Nonlinear dynamics of a magnetization subject to rf feedback field: new experimental evidence, C.R. Chimie 7 (2004) 329–333.
[26] M.P. Augustine, E.H. Hahn, Three component spin echoes generated by radiation damping, J. Chem. Phys. 107 (1997) 3224–3228.
[27] Copyright 1989-2005. INRIA ENPC,www.scilab.org, Scilab, a free scientific software package.
[28] H.T. Edzes, The nuclear magnetization as the origin of transient changes in the magnetic field in pulsed NMR experiments, J. Magn. Reson. 86 (1990) 293–303.
[29] H.G. Schuster, Deterministic Chaos: An Introduction, VCH Publishers, 1989.